Characterizing the Low-Mass Molecular Component in the Northern Small Magellanic Cloud

Muller, E.[1*], Ott, J.[2†], Hughes, A.[3], Pineda, J.L.[4], Wong, T.[4], Mizuno, N.[1], Kawamura, A.[1], Mizuno, Y.[1], Fukui, Y. [1], Onishi, T.

[1] Nagoya University, Japan. email: erik@a.phys.nagoya-u.ac.jp. [2] National Radio Astronomy Observatory, USA. [3]Swinburne University of Technology, Australia. [4]Jet Propulsion Laboratory/California Institute of Technology, USA and [5]University of Illinois, USA.

*JSPS Fellow (Nagoya University), †Jansky Fellow (NRAO)

Abstract:

As part of the SMC component of the MAGMA project (see also posters by Hughes and Wong), three molecular complexes in the north SMC are mapped with the Mopra telescope. We have resolved large, contiguous regions into cloud complexes of up to 6 cores. These observations show that the weaker molecular clouds in the north of the SMC conform to existing empirically-related properties of their counterparts in the south-west of the SMC, while at the same time showing significantly narrower line-widths for their estimated radii.

Importantly, We find that the observed molecular emission does not always correlate well with dust emission, as observed at 70 and 160 microns. We also identify two examples where molecular material is distributed over two distinct and widely separate velocity ranges within closely spaced lines of sight, suggesting the action of an energetic process sometime in the history of the SMC which has caused the two components to accelerate apart.

Observations:

We focused on selected regions in the north of the SMC, shown as boxed regions towards the top of Figure 1, labelled NE-1, NE-3 and a newly-named region: NE-4 (following Rubio et al, 1986). The observations were made with the Mopra Telescope, in NSW, Australia. The UNSW-MOPS broadband backend system was used in the high-resolution mode, configured to the 12CO(J=1-0) transition at 115.27 GHz.

The data were processed using the LIVEDATA and GRIDZILLA processing software. Smoothing the data slightly results in an RMS level of 210 mK, a beamsize of 42” (12 pc).

Figure 1, Below:
Neutral Hydrogen (HI) of the SMC (colour scale; Stanimirovic 2000). The contours show the 300 mK and 900 mK peak brightness level of the CO(J=1-0) transition as measured by NANTEN (Mizuno et al, 2000). The boxes indicate the three regions reported here, although a number of other notable molecular regions are also being observed. The heavy dotted circle roughly defines molecular clouds in the north of the SMC, while the dashed circle roughly defines molecular clouds in the south-west SMC, which were observed extensively with SEST (e.g. Rubio et al.1993, and papers in that series).

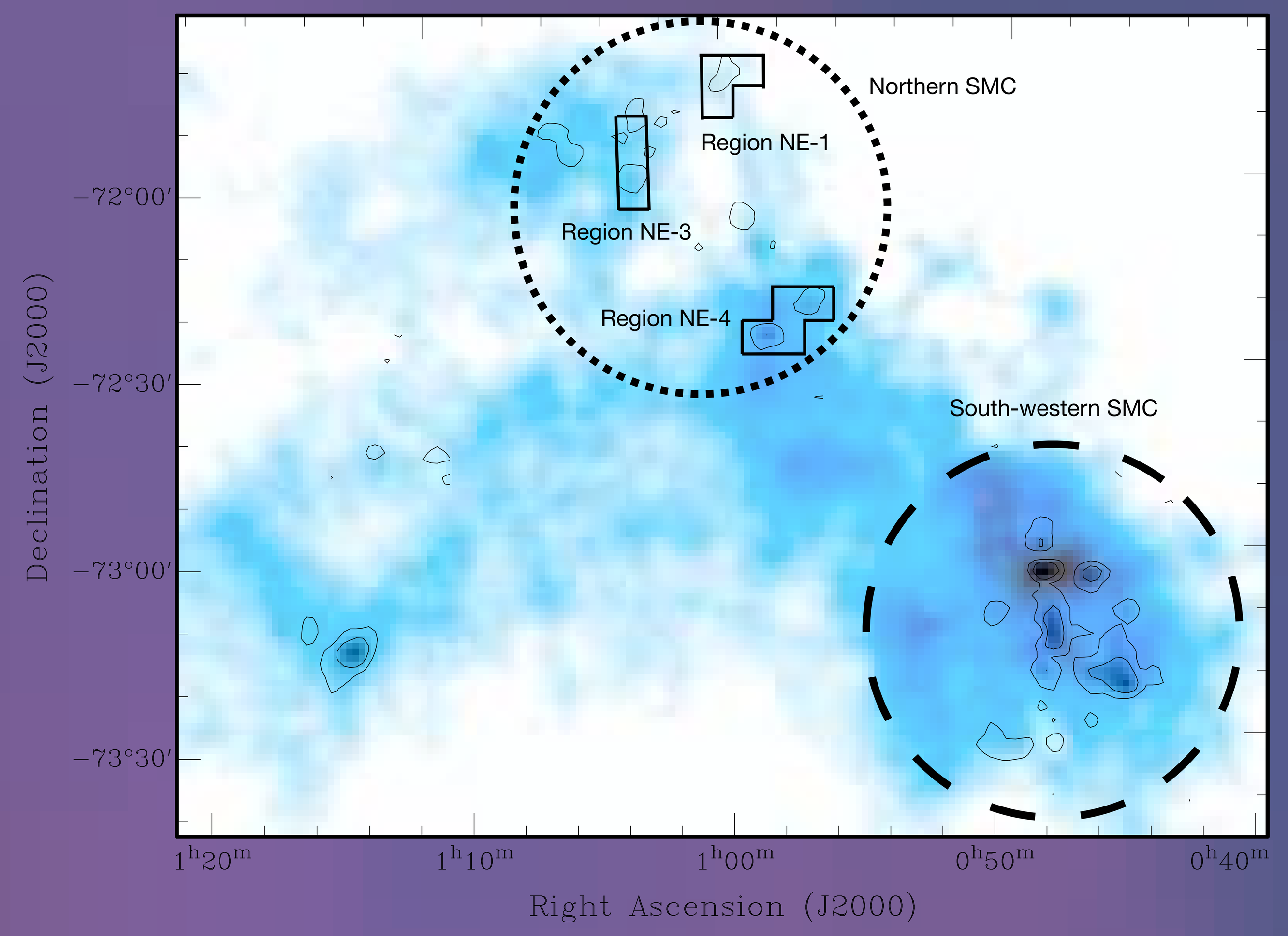

Figure 2, Colour images, Below and Left:
The three mapped regions, NE-1, NE-3, and the newly-named NE-4 are shown overlaid on Spitzer 24, 70 and 160 μm maps (Bolatto et al, 2007). Spectra containing CO emission, detected by CLOUDPROPS (rosolowsky et al, 2000) are shown with contours of integrated brightness (0.5+1 K). Peaks of emission are labelled and characterised. CO cloud data points are plotted in Figure 5. We see that usually, the brightest peaks of CO are associated with μm emission, but this is not always the case, or the association is unclear (e.g. NE3-d, NE-3b). NE-4 (left, lower) shows red and blue contour sets, corresponding to the integrated low and high velocity peaks, respectively.

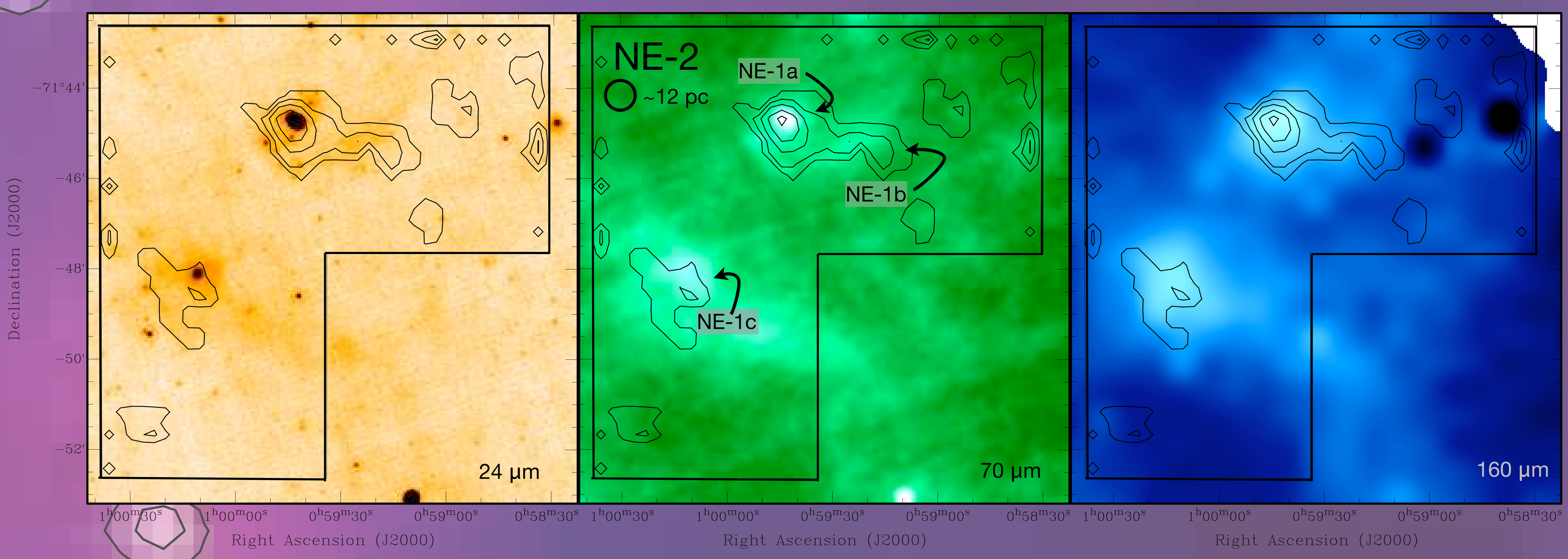

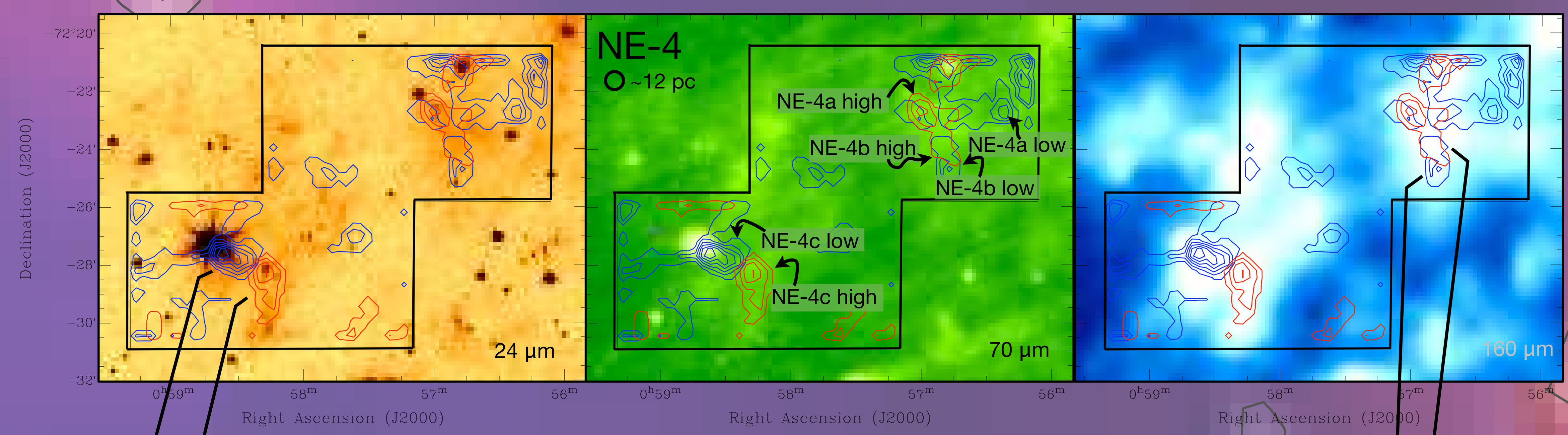

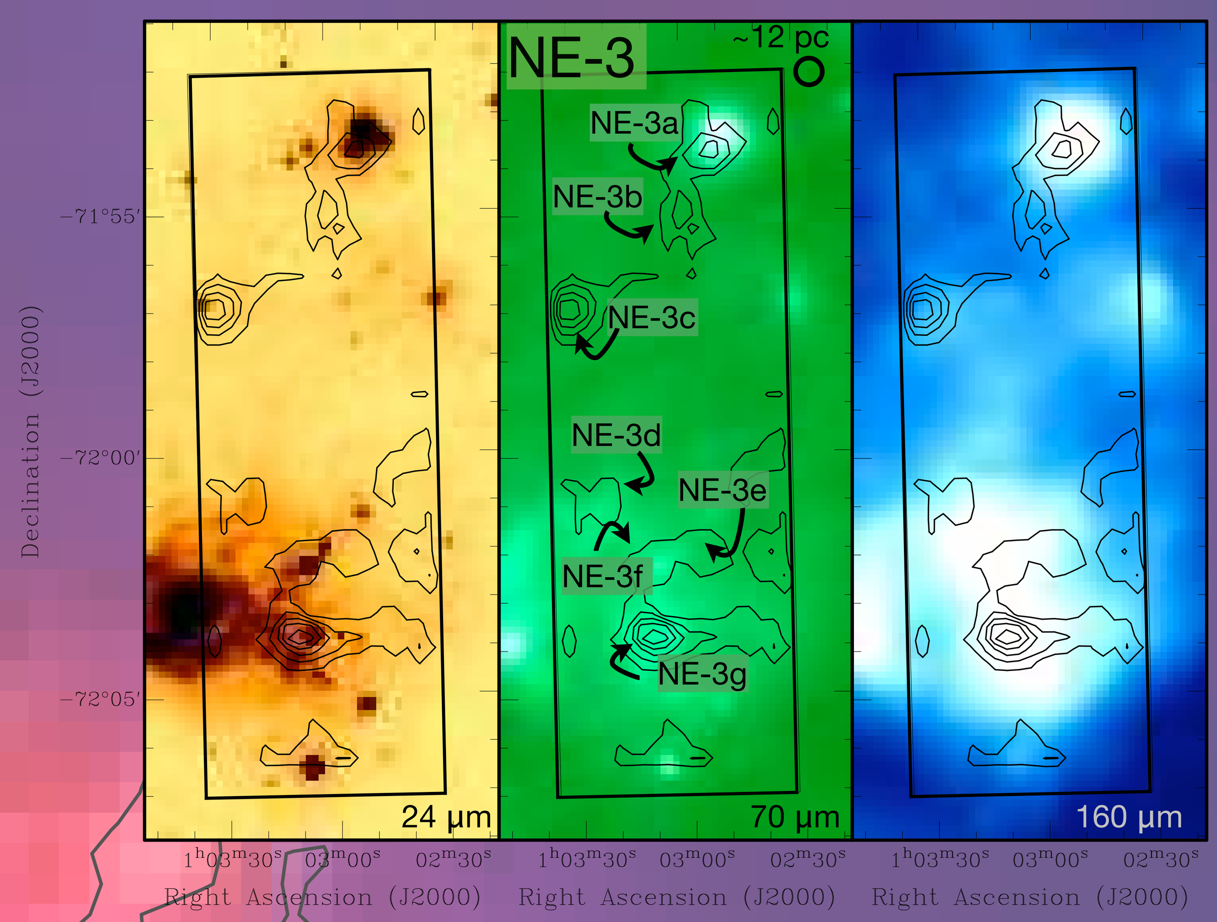

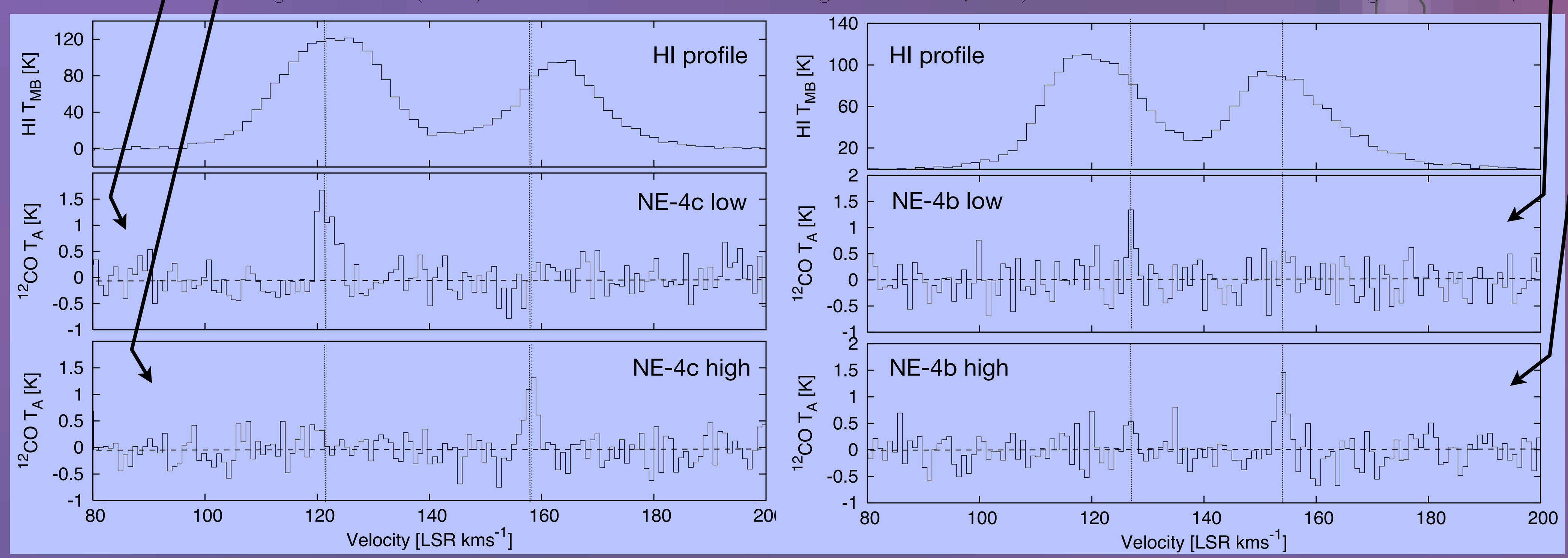

Figure 3, Above:
Spectra of NE-4c, NE-4b, high and low velocity components. Vertical lines locate peak centroids, and their corresponding position in the HI emission profile. Horizontal dotted lines highlight the zero emission.
We see that in both cases, the high/low velocity pairs correspond well with the peaks of HI emission, suggesting a co-evolution of the two phases.

Figure 4, Below:
Parameters of CO clouds in the North SMC (Triangles), measured by Mopra (42” beam) and clouds in the South-west SMC (Diamonds), measured by SEST (45” beam). We find a consistently robust correlation of the luminosity, virial mass and line-width of the two populations, however the northern clouds appear to be somewhat narrow in line-width for their size. Over plotted lines show empirical fits, made by Rubio et al (1996).
We see that the SMC/LMC populations are similar, however the line-widths of the LMC population (Crosses) is somewhat broader. Neither data sets conform to the canonical Larson profile.

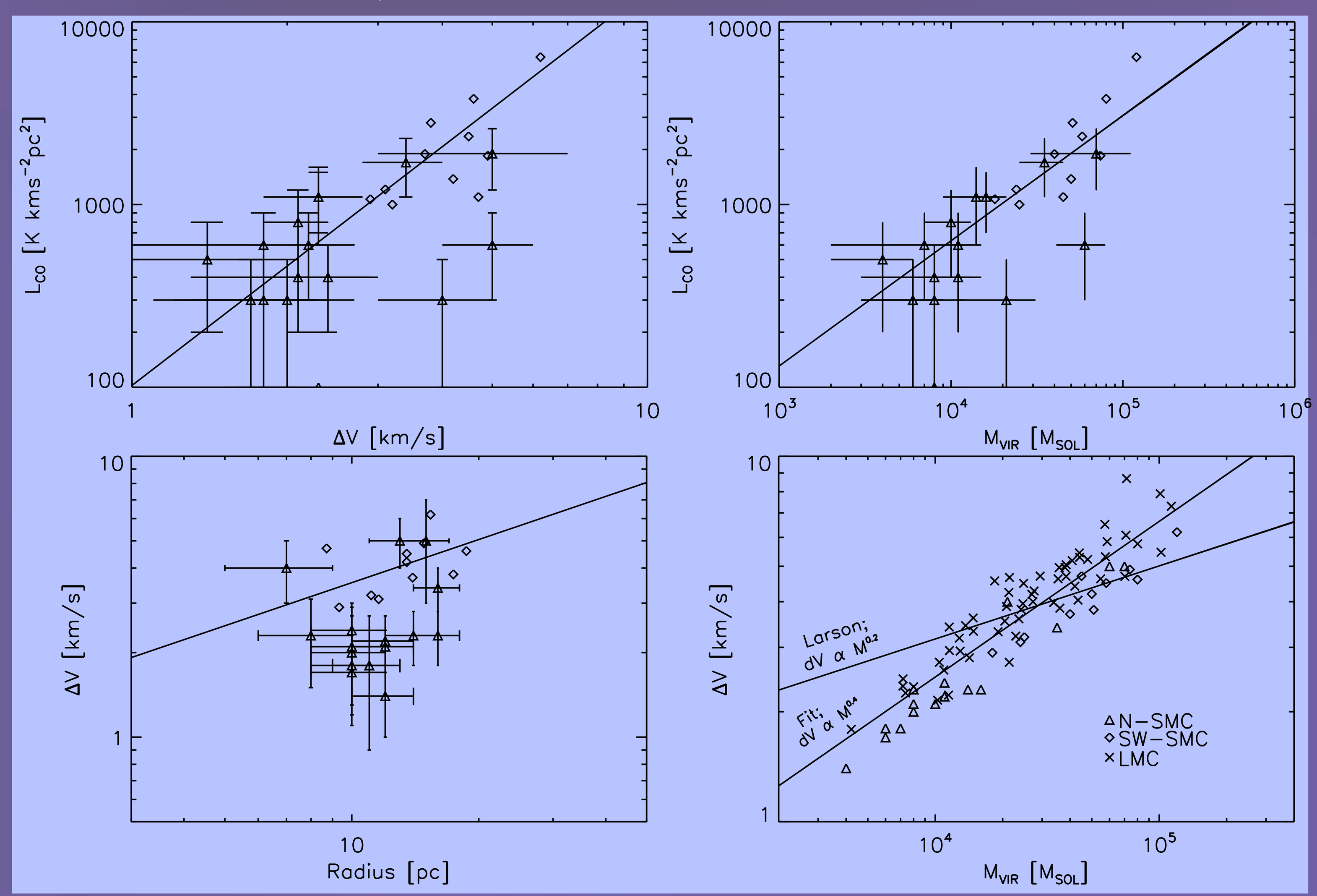

Processing and Analysis:

Clouds were detected using the clump-finding algorithm CLOUDPROPS (Rosolowsky et al 2006). Detected clumps were measured and characterised *by eye only* - i.e. the output parameters of CLOUDPROPS were not used in cloud characterisation. Gaussian fits were made using Gnuplot, and the reported errors were found to be more conservative than those using statistical algorithms, such as Landman, Roussel-Dupre & Tanigawa (1982).
Shown in Figure 2 (colour maps) is the integrated CO brightness for only spectra containing emission for each region (identified by CLOUDPROPS, and all other datapoints are set to zero).
We estimate the viral mass with $M_{VIR} \approx 190\, R\Delta V^2$, which enables us to estimate the H_2-to-CO conversion factor with $X_{CO} \approx M_{VIR}/L_{CO}$.

Results:

A bimodal CO profile has been detected for the first time in the SMC, shown in figure 3. Such alignment is consistent with the HI profile and suggests some energetic process driving the bimodality.
Figure 4 shows the basic parameters for the detected peaks within the northern SMC, compared with the CO clouds in the southwest SMC, as measured by the SEST telescope, at a comparable beam size (Rubio et al, 1996). Here we find that the luminosities, virial masses and line-widths are generally comparable, however the norther clouds appear to have a relatively narrow velocity dispersion for their radii.
We also compare the SMC CO cloud population to the LMC cloud population, and find that the populations overlap in virial mass and line-width, but that the SMC CO cloud population have smaller median masses and smaller line widths, consistent for a less enriched ISM which is forming stars less actively.

Conclusions:

1. The X factor we calculate for the northern SMC CO cloud population is 1.2×10^{21}, this value is broadly consistent with earlier estimates made for the south east population (Rubio et al. 1993), and is approximately an order of magnitude higher than the X factor calculated for the LMC (Pineda et al, in prep).
2. We find that the CO cloud population in the northern SMC is significantly different to that of the southwest, in terms of its velocity/radius properties. This implies that the properties of the ISM between the two regions is also different, in some as-yet unquantified way. We notice that a difference is reflected also in the general properties of the HII regions (from data collated by Bica et al, 2008), where the northern SMC shows a relative deficiency of small-radii HII regions.
3. Micron brightness is regarded as a proxy for an underlying molecular component (e.g. Leroy et al, 2007), and associating CO emission directly with micron emission and with the more global molecular fraction certainly comes with caveats (e.g. Bot et al, 2007). We find that the spatial correlation of detected CO and regions of bright micron emission is not robust, and even cooler micron wave-lengths will not always correlate with detected CO. Mass estimates made using micron data sets may underrepresent the mass of CO, and therefore, the total molecular component.
4. The distribution of CO within the north of the SMC has some unexpected morphology - the fact that the CO emission profiles are bimodal suggests that some energetic process has occurred, or is still in action. Multi-wavelength data of this part of the SMC does not clearly suggest any specific scenario, the simplest assumption involves the action of stellar winds, which have acted to bifurcate the ISM where the CO is present.

Background image:
3-colour image of the northern SMC: Red, blue and green colour scales are 160um Spitzer measurements (Bollato et al.), HI integrated intensity (Stanimirovic et al) and CO integrated intensity, respectively.